Article

#-Borane Complexes of Iridium: Synthesis and Structural Characterization

Travis J. Hebden, Melanie C. Denney, Vincent Pons, Paula M. B. Piccoli, Thomas F. Koetzle, Arthur J. Schultz, Werner Kaminsky, Karen I. Goldberg, and D. Michael Heinekey

J. Am. Chem. Soc., **2008**, 130 (32), 10812-10820 • DOI: 10.1021/ja801898m • Publication Date (Web): 22 July 2008

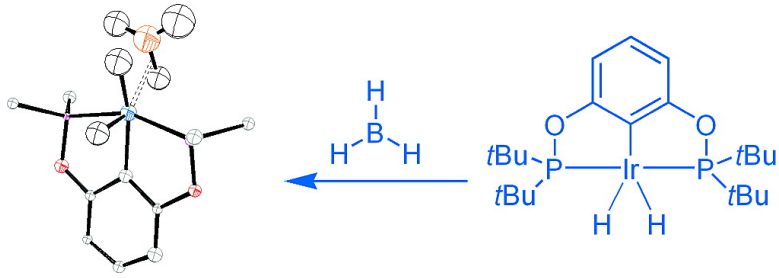

More About This Article

Additional resources and features associated with this article are available within the HTML version:

- Supporting Information
- Links to the 2 articles that cite this article, as of the time of this article download
- Access to high resolution figures
- Links to articles and content related to this article
- Copyright permission to reproduce figures and/or text from this article

View the Full Text HTML

J|A|C|S
ARTICLES

Published on Web 07/22/2008

σ-Borane Complexes of Iridium: Synthesis and Structural Characterization

Travis J. Hebden,[†] Melanie C. Denney,[†] Vincent Pons,[†] Paula M. B. Piccoli,[‡] Thomas F. Koetzle,[‡] Arthur J. Schultz,[‡] Werner Kaminsky,[†] Karen I. Goldberg,[†] and D. Michael Heinekey[†,*]

Department of Chemistry, University of Washington, Box 351700, Seattle, Washington 98195-1700, and Intense Pulsed Neutron Source, Argonne National Laboratory, Argonne, Illinois 60439

Received March 18, 2008; E-mail: heinekey@chem.washington.edu

Abstract: Reaction of $NaBH_4$ with (*t*BuPOCOP)IrHCl affords the previously reported complex (*t*BuPOCOP)-$IrH_2(BH_3)$ (**1**) (*t*BuPOCOP = κ^3-C_6H_3-1,3-[OP(*t*Bu)$_2$]$_2$). The structure of **1** determined from neutron diffraction data contains a B−H σ-bond to iridium with an elongated B−H bond distance of 1.45(5) Å. Compound **1** crystallizes in the space group $P\bar{1}$ ($Z = 2$) with $a = 8.262$ (5) Å, $b = 12.264$ (5) Å, $c = 13.394$ (4) Å, and $V = 1256.2$ (1) Å^3 (30 K). Complex **1** can also be prepared by reaction of BH_3·THF with (*t*BuPOCOP)IrH_2. Reaction of (*t*BuPOCOP)IrH_2 with pinacol borane gave initially complex **2**, which is assigned a structure analogous to that of **1** based on spectroscopic measurements. Complex **2** evolves H_2 at room temperature leading to the borane complex **3**, which is formed cleanly when **2** is subjected to dynamic vacuum. The structure of **3** has been determined by X-ray diffraction and consists of the (*t*BuPOCOP)Ir core with a σ-bound pinacol borane ligand in an approximately square planar complex. Compound **3** crystallizes in the space group $C2/c$ ($Z = 4$) with $a = 41.2238$ (2) Å, $b = 11.1233$ (2) Å, $c = 14.6122$ (3) Å, and $V = 6700.21$ (19) Å^3 (130 K). Reaction of (*t*BuPOCOP)IrH_2 with 9-borobicyclononane (9-BBN) affords complex **4**. Complex **4** displays ^{1}H NMR resonances analogous to **1** and exists in equilibrium with (*t*BuPOCOP)IrH_2 in THF solutions.

Introduction

Tridentate ligands containing two phosphine donors that enforce meridional coordination geometries are known as pincer complexes. Such ligands form a wide variety of metal complexes and have been studied extensively.[1,2] The high thermal stability of the tridentate meridional ligand binding has allowed application of such complexes in a wide range of reactions, including the activation of C−H bonds at high temperatures. For example, Kaska, Jensen and co-workers reported that (*t*BuPCP)IrH_2 (*t*BuPCP = κ^3-C_6H_3-1,3-[CH_2P(*t*Bu)$_2$]$_2$) Chart 1, left) is an effective catalyst for transfer dehydrogenation of alkanes.[3,4] The reaction is carried out at 200 °C, but the catalyst is robust. Subsequently, it was reported by Jensen and co-workers and by Brookhart and co-workers that (R_2POCOP)IrH_2 (R_2POCOP = κ^3-C_6H_3-1,3-[OP(R)$_2$]$_2$ where R = *i*Pr, *t*Bu) (Chart 1, right) is a more active catalyst, allowing for dehydrogenation at lower temperatures.[5−7] This alkane dehydrogenation has been combined with metathesis of the resulting alkenes by Goldman, Brookhart and co-workers in an elegant demonstration of tandem catalysis that has been termed *alkane metathesis*.[8]

Chart 1

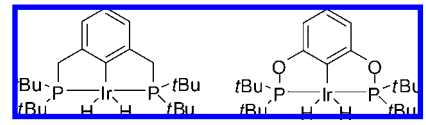

Recently we have reported that (*t*BuPOCOP)IrH_2 is a very effective catalyst for the dehydrogenation of ammonia borane (AB) at room temperature.[9] Ammonia borane is a material with considerable promise as a hydrogen storage material.[10−12]

$$n\mathrm{H_3NBH_3} \overset{\text{[catalyst]}}{\rightleftharpoons} [\mathrm{H_2NBH_2}]_n + n\mathrm{H_2}$$

[†] University of Washington.
[‡] Argonne National Laboratory.

(1) van der Boom, M. E.; Milstein, D. *Chem. Rev.* **2003**, *103*, 1759–1792.
(2) Albrecht, M.; van Koten, G. *Angew. Chem., Int. Ed.* **2001**, *40*, 3750–3781.
(3) Gupta, M.; Hagen, C.; Flesher, R. J.; Kaska, W. C.; Jensen, C. M. *J. Chem. Soc., Chem. Comm.* **1996**, 2083–2084.
(4) Gupta, M.; Hagen, C.; Kaska, W. C.; Cramer, R. E.; Jensen, C. M. *J. Am. Chem. Soc.* **1997**, *119*, 840–841.
(5) Morales-Morales, D.; Redón, R.; Yung, C.; Jensen, C. M. *Inorg. Chim. Acta* **2004**, *357*, 2953–2956.
(6) Göttker-Schnetmann, I; White, P.; Brookhart, M *J. Am. Chem. Soc.* **2004**, *126*, 1804–1811.
(7) Göttker-Schnetmann, I.; White, P. S.; Brookhart, M. *Organomet.* **2004**, *23*, 1766–1776.
(8) Goldman, A. S.; Roy, A. H.; Huang, Z.; Ahuja, R.; Schinski, W.; Brookhart, M. *Science* **2006**, *312*, 257–261.
(9) Denney, M. C.; Pons, V.; Hebden, T. J.; Heinekey, D. M.; Goldberg, K. I. *J. Am. Chem. Soc.* **2006**, *128*, 12048–12049.
(10) U. S. Department of Energy *Basic Research Needs for the Hydrogen Economy*; http://www.sc.doe.gov/bes/hydrogen.pdf.
(11) Marder, T. B. *Angew. Chem., Int. Ed.* **2007**, *46*, 8116–8118.
(12) Stephens, F. H.; Pons, V.; Baker, R. T. *J. Chem. Soc., Dalton Trans.* **2007**, 2613–2626.

10.1021/ja801898m CCC: $40.75

A gradual decrease in the rate of dehydrogenation was noted, and ultimately attributed to the formation of a catalytically dormant species, formulated as (*t*BuPOCOP)IrH$_2$(BH$_3$) (**1**). We now report further investigations of complex **1** and related iridium species resulting from interaction of boranes and borohydrides with the iridium center.

Results

Preparation and Spectroscopic Characterization of Complex 1. Reaction of $NaBH_4$ with (*t*BuPOCOP)IrHCl affords the previously reported complex (*t*BuPOCOP)IrH$_2$(BH$_3$) (**1**)[9] (*t*BuPOCOP = κ^3-C$_6$H$_3$-1,3-[OP(*t*Bu)$_2$]$_2$). Complex **1** can also be prepared by reaction of BH$_3$·THF with (*t*BuPOCOP)IrH$_2$ (equation 1).

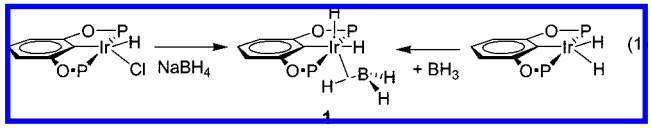

Complex **1** is stable and can be isolated at room temperature. The ^{1}H NMR spectrum of complex **1** exhibits two sets of tertiary butyl resonances and appropriate aromatic resonances expected for the POCOP ligand. Also observed was a sharp triplet at −20.7 ppm (J_{HP} = 12 Hz) and two broad resonances at −5.4 and −6.6 ppm each integrating roughly to one proton. A very broad signal was observed at 7.0 ppm which integrated to two protons. At low temperature (240 K) the line widths of the broad resonances are significantly reduced, while the resonance at −20.7 ppm is shifted to −20.4 ppm and observed as a quartet (J = 12 Hz) at an observation frequency of 500 MHz. The assignment of the broad resonances as BH moieties was confirmed by independent synthesis of a selectively deuterated compound **1-*d*$_4$**, by reaction of (*t*BuPOCOP)IrHCl with $NaBD_4$. The ^{2}H NMR spectrum of **1-*d*$_4$** displayed resonances at 7.0, −5.4, −6.6 and −20.7 ppm, confirming the assignment given for the ^{1}H NMR spectrum. Above room temperature the resonances at 7.0 and −5.4 ppm broaden into the baseline followed by broadening of the resonance at −6.6 ppm. At the highest observed temperature (353 K) the triplet at −20.7 ppm remains sharp. Variable temperature (VT) ^{1}H NMR spectra of complex **1** are contained in the Supporting Information. The quartet resonance at −20.4 ppm in the low temperature (240 K) ^{1}H NMR spectrum collapses to a doublet (J = 11 Hz) in the ^{1}H{^{31}P} NMR spectrum. In homonuclear decoupling experiments, the quartet resonance collapses to a triplet (J = 12 Hz) when the resonance at −5.4 ppm is selectively irradiated; however, irradiation of the resonance at −6.6 ppm has no effect on the line shape of the resonance at −20.4 ppm.

The measured T_1(min) values for the resonances at 7.0, −5.4, −6.6 and −20.4 ppm are 82, 110, 129, and 360 ms, respectively. Minima were recorded at 210 K for all resonances. The IR spectrum of **1** (see Supporting Information) exhibits bands expected for POCOP iridium complexes, as well as bands at 2462, 2439, 2292, 2224 and 1933 cm^{-1} which are attributed to B−H and Ir−H stretching modes.

Solid State Structure of Complex 1. The structure of complex **1** has been determined by neutron diffraction. The data collection and refinement parameters are summarized in the Supporting Information. Details of the structure determination are given in the Experimental Section. An ORTEP diagram of the structure of **1** is shown in Figure 1.

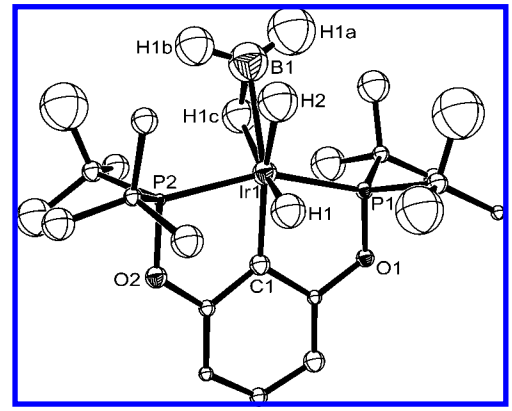

Figure 1. ORTEP diagram of the structure of **1** at 30 K. Hydrogen atoms other than those in the coordination sphere of the Ir and B atoms have been omitted for clarity. Ellipsoids are shown at 50% probability. Selected bond distances (Å): Ir1−B1 2.37(3); Ir1−H1 1.61(4); Ir1−H2 1.74(4); Ir1−H1c 1.90(4); B1−H1c 1.45(5); B1−H2 1.74(5). Selected bond angles (°): H1−Ir1−H1c 167.0(18); H2−B1−H1c 100.3(26) Ir1−H1cB1 89(2). An extended list of bond distances and angles can be found in the Supporting Information.

Chart 2

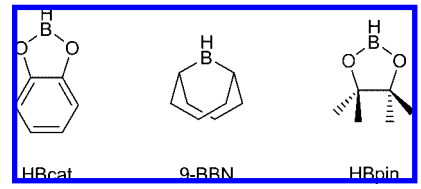

Reactivity of Complex 1. Complex **1** is thermally robust, exhibiting no discernible reaction upon heating to reflux in benzene or hexane. When a THF solution of **1** was exposed to H_2 (30 psi) at room temperature, (*t*BuPOCOP)IrH$_2$ was observed along with the "tetrahydride" complex (*t*BuPOCOP)IrH$_4$.[7] When complex **1** is maintained at a temperature of 120 °C for a period of 12 h or longer, decomposition occurs to (*t*BuPOCOP)IrH$_2$, (*t*BuPOCOP)IrH$_4$, and several other unidentified products.

Preparation of Other B−H Adducts. Boranes previously reported to form complexes with transition metals include catecholborane (HBcat), 9-borobicyclononane (9-BBN), and pinacolborane (HBpin) (Chart 2).[13]

In the expectation of preparing analogs of complex **1**, we have explored reaction of these boranes with (*t*BuPOCOP)IrH$_2$. Reaction of (*t*BuPOCOP)IrH$_2$ with a THF solution of HBpin at 0 °C resulted in clean formation of an HBpin complex, designated as complex **2**. The ^{1}H NMR spectrum of **2** at room temperature displays a very broad resonance at −9.8 ppm with an integrated intensity corresponding to three hydrogen atoms. The variable temperature ^{1}H NMR spectra of **2** (Figure 2) display two coalescence events, one at ∼196 K and the other at ∼304 K.

Solutions of complex **2** at room temperature slowly evolve hydrogen and form a new complex **3**, which exhibits a single broad resonance in the ^{1}H NMR spectrum at −13.15 ppm with an integrated intensity corresponding to one hydrogen atom.

Complex **3** can be generated cleanly by subjecting solutions of complex **2** to dynamic vacuum for a period of several hours at room temperature. The upfield resonance sharpens consider-

(13) Lachaize, S.; Essalah, K.; Montiel-Palma, V.; Vendier, L.; Chaudret, B.; Barthelat, J.-C.; Sabo-Etienne, S. *Organometallics* **2005**, *24*, 2935–2943.

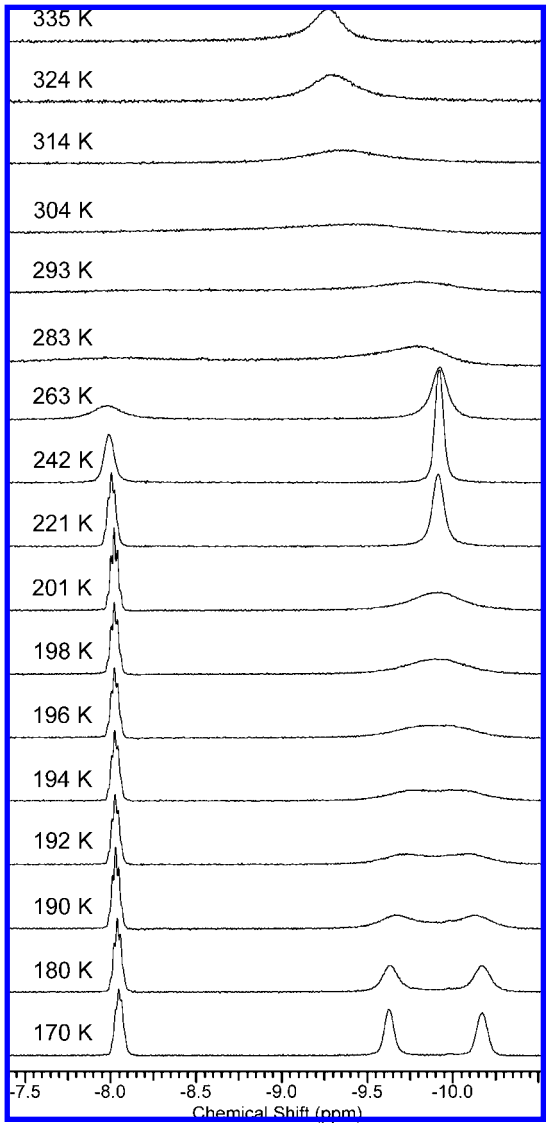

Figure 2. Partial (high field region) $^1H\{^{11}B\}$ NMR spectrum (500 MHz, THF-d_8) of **2** as a function of temperature.

ably in the $^1H\{^{11}B\}$ NMR spectrum, indicating that this H atom is closely associated with a boron atom. The IR spectrum of **3** displays a band at 2014 cm^{-1} which is assigned to the B−H stretch. Crystals of **3** suitable for X-ray diffraction were obtained by slow evaporation of a THF solution. The structure obtained is shown in Figure 3. Crystal data and structure refinement parameters are summarized in the Supporting Information.

Reaction of $[Na]^+[H\text{-}9\text{-}BBN]^-$ with (*t*BuPOCOP)IrHCl resulted predominantly in formation of the known complex $[NA]^+[(tBuPOCOP)IrH_3]^{-7}$ and Cl-9-BBN with small amounts of (*t*BuPOCOP)IrH_2, (*t*BuPOCOP)IrH_4 as well as a new product (*t*BuPOCOP)IrH_3-9-BBN (**4**). Reaction of (*t*BuPOCOP)IrH_2 with a THF solution of 9-BBN resulted in formation of **4** predominantly. This reaction did not go to completion even with excess (3 equivalents) 9-BBN. Complex **4** displays three broad resonances in the upfield region of the ^1H NMR spectrum. Two broad singlets are observed at −6.0 and −7.4 ppm and an apparent 1:3:3:1 quartet centered at −21.32 ppm, each resonance integrating to one proton. In the $^1H\{^{31}P\}$ NMR spectrum the quartet collapses to a doublet with $J = 12$ Hz. When the resonance at −6.0 is selectively decoupled in the ^1H spectrum, the quartet collapses to a triplet (1:2:1) with $J = 12$ Hz. Selective

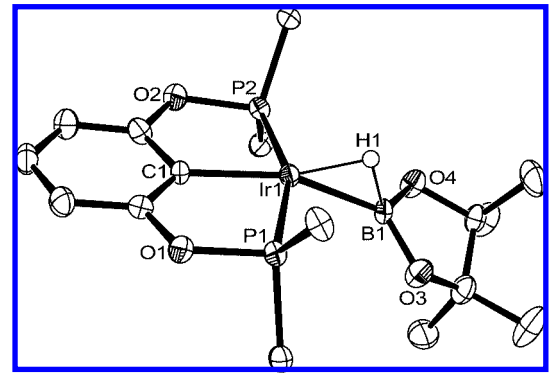

Figure 3. ORTEP diagram of **3** at 120 K with thermal ellipsoids at 50% probability. H atoms (with the exception of H1) and methyl carbons of the *t*butyl groups are omitted for clarity. Selected bond distances (Å): Ir1−B1 2.082(5): Ir1-center of B1−H1 bond 1.61(6). Selected bond angles (°): C1−Ir1−H1 160(2); C1−Ir1-center of B1−H1 bond 177(2); C1−Ir1−B1 155.6(2). An extended list of bond distances and angles is included in the Supporting Information.

Scheme 1

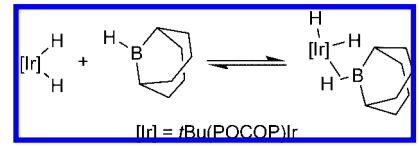

decoupling of the resonance at −7.4 ppm has no effect on the resonance at −21.32 ppm. This scalar coupling was also observed in a ^1H COSY experiment.

A spin saturation transfer experiment in which the residual (*t*BuPOCOP)IrH_2 resonance at −17.21 ppm is irradiated results in a loss of intensity for the shift located at −21.32 ppm. Observing the upfield region of the reaction of 9-BBN with (*t*BuPOCOP)IrH_2 at variable temperature reveals that at lower temperatures, the signal intensity of (*t*BuPOCOP)IrH_2 decreases relative to that for complex **4**. This equilibrium (illustrated in Scheme 1) was observed as a function of temperature and is displayed in a van 't Hoff plot in the Supporting Information.

Discussion

Complex **1** was initially obtained in the course of our studies of AB dehydrogenation catalyzed by (*t*BuPOCOP)IrH_2. When this reaction is carried out under conditions where the hydrogen can readily escape, catalytic activity gradually declines due to the formation of a dormant species, ultimately identified as complex **1**. Two independent synthetic approaches for the preparation of complex **1** have been developed (eq 1), the most convenient being the reaction of $NaBH_4$ with (*t*BuPOCOP)IrHCl.

Given this synthetic approach, it seemed reasonable to consider complex **1** to be a borohydride (BH_4^-) adduct of the cationic, formally sixteen electron moiety $[(tBuPOCOP)IrH]^+$. Based on extensive literature precedents, several different binding modes for borohydride interactions with the iridium center would be possible.[14,15] An alternative description is to consider the complex to be a BH_3 adduct of the neutral sixteen electron species (*t*BuPOCOP)IrH_2. These possibilities are depicted below in Chart 3.

(14) Marks, T. J.; Kolb, J. R. *Chem. Rev.* **1977**, *77*, 263–293.
(15) Makhaev, V. D. *Russ. Chem. Rev.* **2000**, *69*, 727–746.

Chart 3. Possible Structures for Complex **1**; Ir = (*t*BuPOCOP)Ir

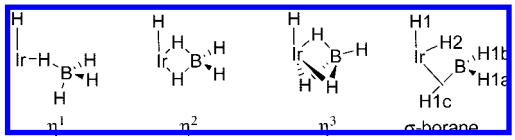

Table 1. Calculated and Observed T_1(min) Values for Non-Ligand H Nuclei in Complex **1**

atom	calculated T_1(min) (ms)	δ_H (ppm)	observed T_1(min) (ms)
H2	283	−6.6	129
H1c	198	−5.4	110
H1a/H1b	136	7.0	82

Observation of the ^{1}H NMR spectrum of **1** at room temperature is hampered by the broad resonances observed for H atoms bound to B, due to rapid relaxation caused by the quadrupolar boron nucleus. Lowering the observation temperature to 240 K gives sharper lines, although three of the four resonances are still significantly broadened by the boron nucleus. The sharp resonance at −20.4 ppm is assigned to H1 based on the lack of line broadening caused by boron. The resonance at +7.0 ppm integrates to two H atoms allowing assignment as H1a/H1b. The occurrence of a resonance at +7.0 ppm seems surprising, but similar chemical shifts have been previously reported for related Ir complexes.[16,17] The resonances at −5.4 ppm and −6.4 ppm are assigned to H1c and H2, respectively.

The assignments were confirmed by measurement of relaxation times. Hydrogen atoms directly attached to B relax rapidly as the proximity of the boron nucleus contributes significantly to the relaxation. We can apply the method described by Halpern and co-workers[18] as a means of qualitative assignment of the ^{1}H resonances.

Estimated values for T_1(min) can be made using the structure derived from neutron diffraction data and the equations detailed in the work of Halpern and co-workers. The use of relaxation rates ($R = [T_1(\text{min})]^{-1}$) is preferred for this analysis as these values are additive. All relaxation rates for various nuclei have been previously given except for the boron nuclei. These values were calculated as 15.94 Å^6 s$^{-1}/r^6$ for ^{10}B (18.8% natural abundance) and 9.219 Å^6 s$^{-1}/r^6$ for ^{11}B (81.2% natural abundance). Using this method we are able to assign qualitatively the resonances observed in the ^{1}H NMR spectrum of **1**, shown in Table 1.

These assignments were also verified by the preparation of **1-*d*$_4$** by reaction of (*t*BuPOCOP)IrHCl with $NaBD_4$. Deuterium NMR spectroscopy verifies that the assignment outlined above is correct. The deuterium is distributed through all hydridic and B−H positions in **1-*d*$_4$**, suggesting that there is a dynamic process operational in complex **1** that can facilitate site exchange. This dynamic process is slow on the NMR time scale, since separate resonances are observed for H1, H2, H1c and H1a/H1b, but exchange on the laboratory time scale serves to scramble the D label through all four sites. Since the hydridic proton present in (*t*BuPOCOP)IrHCl originates from the *ipso* position on the naked ligand, a maximum of only 80% deuterium incorporation is possible. A suggested mechanism for the exchange of hydridic H atoms and H atoms associated with a BH_4^- ligand has been previously discussed in the literature.[19] This combined computational and experimental study concluded that exchange of these sites occurred via an intramolecular mechanism.

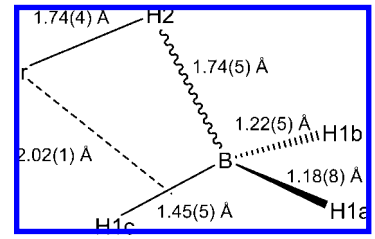

Figure 4. Interatomic distances of atoms near Ir and B in complex **1**, taken from neutron diffraction analysis.

The assignments of atoms H1c and H2 to resonances at −5.4 and −6.6 respectively is consistent with the idea that the more activated of the BH bonds (that with more bonding character to Ir) will be that which is more stabilized and therefore less likely to participate in exchange with the H1a/H1b protons. In this vein, H1c with a B−H distance of 1.45(5) Å would be more easily exchanged with the H1a/H1b atoms than H2 with a B−H distance of 1.74(4) Å. Above room temperature the ^{1}H resonance at −5.4 broadens noticeably at lower temperature than the resonance at −6.6. This difference is, however, very subtle, indicating that exchange barriers among H atoms in proximity to boron are extremely close in energy. At the highest observed temperature the resonance at −5.4 ppm is indistinguishable with the baseline, however the resonance at −6.6 ppm is still obviously present (see Supporting Information). The difference in coalescence temperatures is greater than what would be expected when accounting only for the frequency differences from the resonance at 7.0 ppm, indicating that two separate exchange mechanisms are present. This type of exchange has been proposed for similar structures which contain asymmetrically bound η^2-BH_4^- ligands and a hydride bound to one metal center. Werner and co-workers have an excellent discussion of the exchange mechanism.[20] Several other examples of Ru complexes with similar VT ^{1}H NMR spectral features to that displayed by complex **1** have been reported in the literature, indicating that these complexes may share structural characteristics.[21–23]

The crystal structure of **1** as determined by neutron diffraction is displayed in Figure 1. Selected interatomic distances and bond angles are summarized in Supplementary Table 2 (see Supporting Information). A complete list of bond distances and angles can be found in the Supporting Information. Figure 4 displays a concise summary of the pertinent bond distances for complex **1**.

Although the high background and resulting low data to parameter ratio of the neutron data has resulted in relatively large errors on the bond distances and angles, there is important information to be gleaned from the structure. Complex **1** was

(16) Empsall, H. D.; Mentzer, E.; Shaw, B. L. *J. Chem. Soc., Chem. Comm.* **1975**, 861–862.
(17) Empsall, H. D.; Hyde, E. M.; Mentzer, E.; Shaw, B. L.; Uttley, M. F. *J. Chem. Soc., Dalton Trans.* **1976**, 2069–2074.
(18) Desrosiers, P. J.; Cai, L.; Lin, Z.; Richards, R.; Halpern, J. *J. Am. Chem. Soc.* **1991**, *113*, 4173–4184.
(19) Demachy, I.; Esteruelas, M. A.; Jean, Y.; Lledós, A.; Maseras, F.; Oro, L. A.; Valero, C.; Volatron, F. *J. Am. Chem. Soc.* **1996**, *118*, 8388–8394.
(20) Werner, H.; Esteruelas, M. A.; Meyer, U.; Wrackmeyer, B. *Chem. Ber.* **1987**, *120*, 11–15.
(21) Mazanec, T. J.; Letts, J. B.; Meek, D. W. *J. Chem. Soc., Chem. Comm.* **1982**, 356–358.
(22) Letts, J. B.; Mazanec, T. J.; Meek, D. W. *J. Am. Chem. Soc.* **1982**, *104*, 3898–3905.
(23) Chamberlain, B.; Duckett, S. B.; Lowe, J. P.; Mawby, R. J.; Stott, J. C. *J. Chem. Soc., Dalton Trans.* **2003**, 2603–2614.

initially postulated in our previous study as either a bidentate borohydride complex or as the BH_3 adduct of the precursor iridium hydride complex.[9] Figure 1 illustrates the complex as a σ-bound BH_3 adduct of the parent dihydride complex. The two unactivated B−H bonds, B−H1a and B−H1b, have typical terminal B−H distances of 1.18(8) and 1.22(5) Å, respectively. The B−H1c distance of 1.45(5) Å indicates the presence of a highly activated agostic bond between the BH_3 group and the Ir metal center. The long distance between B1 and H2 (1.74(5) Å) argues against the presence of a BH_4^- ligand, even though the angles around boron are somewhat favorable for such a formulation (see below). The distance between Ir and H1 at 1.61(4) Å is in the normal range for a terminal Ir−H bond; a survey of iridium hydride structures as determined by neutron diffraction gives an average Ir−H distance of 1.580 Å.[24] The Ir−H2 distance of 1.74(4) Å is elongated from this average distance and may indicate a significant interaction between iridium and the electron deficient BH_3 ligand. The Ir−H1c distance of approximately 1.9 Å is too long to be considered a strong interaction. The metal center can be considered to have a distorted octahedral geometry due in part to the restricted geometry imposed by the ancillary pincer ligand and also in part to the resultant crowding of the σ-bound BH_3 around the coordination sites of H2 and H1c.

Diffraction data for tetrahydroborate complexes available in the literature consists mostly of X-ray data in which only the heavy atoms are reliably located. In these cases the binding mode of the tetrahydroborate ligand can sometimes be elucidated using only the M-B interatomic distance. The expected distances for distinguishing between an η^1 or η^2 binding mode are estimated using the Shannon ionic radii of the metal and tetrahydroborate ligand. The iridium atom remains a six coordinate Ir(III) metal center in all considerations, corresponding to a Shannon ionic radius of 0.68 Å.[25] The tetrahydroborate anion sizes based on denticity have been estimated as 1.36 ± 0.06, 1.6 ± 0.1 and >1.8 Å for tri-, bi-, and monodentate binding modes respectively.[26,27] This would translate to Ir−B distances of 2.04, 2.28, and 2.48 Å. An Ir−B distance of 2.37 Å as derived from the neutron diffraction data for **1** would seem to fall in between the monodentate and bidentate binding modes. This is in sharp contrast to the Ir−H2−B angle of 85.8°, which clearly favors an η^2 coordination mode. An η^1 formulation would necessitate that the angle between the metal, bridging hydrogen and boron atom be greater than 90°, allowing the three remaining hydrogen atoms on the boron to be outside of the coordination sphere of the metal. (Previous work by Bau and co-workers displays an excellent example of this type of binding mode in the complex $Cu[P(C_6H_5)_2CH_3]_3(BH_4)$, also characterized using neutron diffraction.)[28] The present analysis would exclude entirely the possible formulation of **1** as a monodentate tetrahydroborate ligand. This seeming discrepancy is resolved in the σ-borane formulation of **1**. The agostic interaction between the Ir and the B−H1c bond would require a closer Ir−B distance than in an η^1 tetrahydroborate structure, while not placing any restraints on an expected Ir−H2−B angle.

Infrared spectroscopy does not provide definitive structural information for these complexes. Terminal B−H modes in an η^1 or η^2 coordinated complex are generally observed between 2300 and 2600 cm^{-1}. The bridging B−H stretches appear as a broad band at 1650 − 2150 cm^{-1} for an η^2 complex and at about 2000 cm^{-1} for an η^1 complex.[15] We propose an alternate analysis, where the band at 2292 cm^{-1} is attributed to the B−H stretch of the B1−H1c bond associated with the Ir center. The bands at 1933 and 2224 cm^{-1} are attributed to the independent stretches of the two Ir−H bonds, although a specific assignment is not made. It may be interesting to note that the tetrahydroborate ruthenium complex reported by Meek and co-workers also did not display IR absorptions that were easily assigned to typical η^1 or η^2 tetrahydroborate complexes.[22]

The position of H2 relative to the BH_3 ligand might possibly be indicative of a highly activated tetrahydroborate complex. However, although the B1−H2 distance of 1.74(5) Å is outside the limits of a bonding interaction and clearly does not support a tetrahydroborate structure model, it appears to be a snapshot of the end product of the addition of tetrahydroborate to a metal to yield a hydride borane complex. Although many tetrahydroborate complexes are known in the literature, compound **1** is the first iridium complex for which the H atoms have been reliably located. The highly activated nature of the B−H2 bond is particularly of interest. For compounds of similar structure there exist two Co compounds with highly activated B−H bonds containing distances of 1.39(9)[29] and 1.38(17)[30] Å, as well as one Nb compound with a B−H distance of 1.39(4) Å.[31] Even these complexes are far from the 1.74(5) Å distance observed in **1**.

At any rate, the characterization of complex **1** as any of the usual transition metal tetrahydroborate complexes (either η^1, η^2, or η^3) is unsatisfactory. Clearly the data presented here do not include any characterizations consistent with the η^3 binding mode. The IR data and structural data are also inconsistent with an η^1 binding mode. Given only these three choices, the description as an η^2 bound BH_4^- ligand would appear to be the closest fit. However, NMR data indicate that this binding mode would at least have to be highly asymmetric in order to agree with observed temperature dependnt spectral lineshapes. As noted above, the structural data derived from our neutron diffraction study indicate that not only is the binding mode asymmetric, but the distance between the B1 and H2 atoms precludes a covalent interaction. Also, the distance between the Ir and B atoms is longer than what would be expected for an η^2 tetrahydroborate complex based on the Shannon ionic radii of the atoms involved. We therefore propose that all data are most consistent with the description of complex **1** as a neutral BH_3 ligand bound to a formally Ir^{III} metal center by a σ-bond interaction involving the Ir and one of the BH bonds.

Complexes in which the BH_3 moiety participates in a σ-bonding interaction with a transition metal have only been reported in cases where the BH_3 ligand is stabilized by an external donor atom.[32] For example, the complex $W(CO)_5(BH_3 \cdot PMe_3)$ reported by Kawano and Shimoi contains a BH σ-bond interaction in which the BH_3 moiety is stabilized by electron donation from the P atom.[33] In the present compound

(24) Allen, F. H. *Acta Cryst. B* **2002**, *58*, 380–388.
(25) Shannon, R. D. *Acta Cryst. A* **1976**, *32*, 751–767.
(26) Edelstein, N. *Inorg. Chem.* **1981**, *20*, 297–299.
(27) Jensen, J. A.; Girolami, G. S. *Inorg. Chem.* **1989**, *28*, 2107–2113.
(28) Takusagawa, F.; Fumagalli, A.; Koetzle, T. F.; Shore, S. G.; Schmitkons, T.; Fratini, A. V.; Morse, K. W.; Wei, C. Y.; Bau, R. *J. Am. Chem. Soc.* **1981**, *103*, 5165–5171.
(29) Nakajima, M.; Saito, T.; Kobayashi, A.; Sasaki, Y. *J. Chem. Soc., Dalton Trans.* **1977**, 385–388.
(30) Dapporto, P.; Midollini, A.; Orlandini, A.; Sacconi, L. *Inorg. Chem.* **1976**, *15* (11), 2768–2774.
(31) Liu, F.-C.; Pleènik, C. E.; Liu, S.; Liu, J.; Meyers, E. A.; Shore, S. G. *J. Organomet. Chem.* **2001**, *627*, 109–120.
(32) Kubas, G. J. In *Metal Dihydrogen and s-Bond Complexes*; Kluwer Academic/Plenum Publishers: New York, 2001; pp 421−429.
(33) Kawano, Y.; Shimoi, M. *Chem. Lett.* **1999**, 869.

Chart 4. Possible Structures for Complex **2**; Ir = (*t*BuPOCOP)Ir

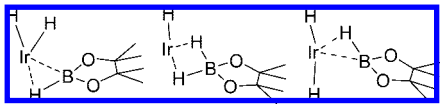

Scheme 2. Two Proposed Exchange Mechanisms Corresponding to the Variable Temperature ^{1}H NMR Spectra of **2**

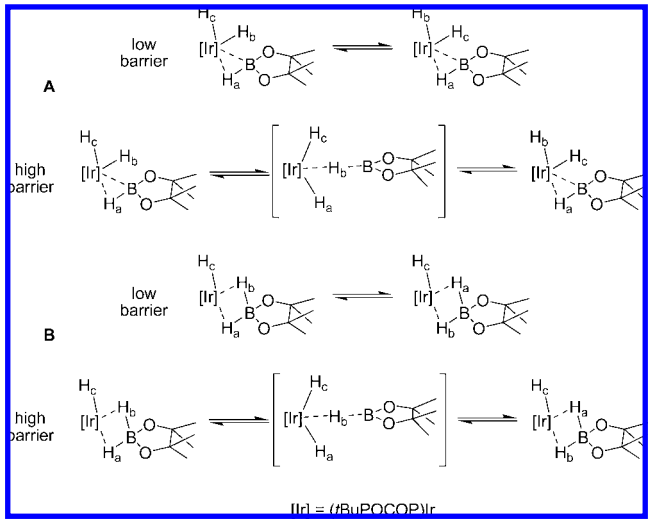

it may be possible that the BH_3 moiety is stabilized by a noncovalent interaction with the adjacent H atom. Although complexes displaying this structure have not been reported in the literature, a similar structure has been computed as being a local minimum in an exchange mechanism for H atoms in hydridic positions and H atoms associated with a tetrahydroborate ligand.[19] In the closely related compound $RuH_2(\eta^2\text{-}HBpin)(\eta^2\text{-}H_2)(PCy_3)_2$, a σ-bound pinacol borane ligand is supported by an adjacent metal-hydride.[13] In this complex the B−H distance of 1.89(2) Å is longer than the 1.74(5) Å in compound **1**, however, this would be expected with the less Lewis acidic pinacol borane ligand.

Clean formation of **2** occurs only at low temperature (~0 °C or lower). Although the original intention was to prepare complexes with analogous structure to complex **1**, it appears that complex **2** differs significantly in reactivity and spectroscopic features. Complex **2** is thermally unstable, releasing H_2 under vacuum quantitatively. The variable temperature ^{1}H NMR of **2** (shown in Figure 2) also highlights these differences.

Three plausible structures for **2** may be considered which are consistent with the ^{1}H NMR spectrum observed at 170 K (depicted in Chart 4). Of these possibilities, the *exo*-σ-borane dihydride (Chart 4, left) and dihydropinacolborate hydride (Chart 4, middle) are favored over the *endo*-σ-borane dihydride (Chart 4, right). It is difficult to imagine a plausible exchange mechanism which would account for the observed spectral features at higher temperatures for the *endo* structure.

These spectral features correspond to fluxionality of the H atoms in proximity to the boron or iridium atoms in the molecule, involving only two protons below 250 K and all three protons above 250 K. Two possible mechanisms for this exchange are illustrated in Scheme 2. In exchange mechanism **A** only one proton is closely associated with the boron atom at low temperature, and the low temperature coalescence corresponds to the rapid exchange of the two hydridic protons. In exchange mechanism **B** two protons are closely associated to the boron atom, and exchange of these protons via rotation of the pinacolborane moiety is responsible for the low temperature event. In both **A** and **B** the high temperature event is postulated as the boron atom dissociating from iridium to be loosely bound through a three center two electron bond mediated by the central hydrogen atom. At the crest of this transition state the plane defined by the iridium, boron and three hydrogen atoms is symmetrical, and the boron may return to its original position or continue on toward the other side of the molecule.

It is unclear which of these two exchange mechanisms would be favored. In complex **1** it is the more hydridic proton which is located upfield relative to the B−H protons in the proton spectrum. Extrapolating this trend for **2** would seem to favor mechanism **A**. At any rate, it is difficult to imagine that rotation of the pinacolborane moiety, as required in mechanism **B**, would occur at low temperature with such ease given the steric environment surrounding the iridium and considering that rotation of the tetrahydroborate ligand in **1** is not observed even at room temperature. It is much more likely that exchange of two sterically less demanding hydrides would occur with relative ease at low temperature.

There are many examples of σ-bonded pinacolborane/hydrido structures reported in the literature.[34–38] Sabo-Etienne and coworkers have studied the coordination modes of many transition metal borane complexes, with direct attention paid to the distinction between a σ-borane and a dihydroborate complex.[13] For ligands in which the dialkoxyborane ligands are not acidic enough to stabilize a dihydroborate structure (as is the case for pinacol) complexes preferentially form σ-borane complexes.

Attempts to derive accurate rate constants for site exchange by fitting the observed spectra to calculated spectra using modeling software were unsuccessful. The broadening observed in the VT NMR spectra is a product of two separate factors: exchange between different proton environments and quadrupolar relaxation of the protons in proximity to the boron nucleus.[39,40] Since a quantitative study of the broadening due to the quadrupolar relaxation was not possible, attempts to elucidate well defined thermal parameters for the exchange events were unsuccessful. Qualitative measures of activation energies are possible if several assumptions are accepted. The low energy process involves two protons. Intermolecular exchange of a pinacol moiety would then involve the brief existence of H_2Bpin^-, which is known to be unstable, forming $Bpin_2^-$ and BH_4^-.[41] Since neither of these species is observed in solution even at high temperatures, we propose that the exchange mechanism is intramolecular, and thus $\Delta S^{\ddagger} \approx 0$. At high temperatures instability of the complex leads to H_2 loss instead of HBpin loss (as observed in ^{1}H NMR spectroscopy) indicating that this process is also intramolecular, and the assumption that $\Delta S^{\ddagger} \approx 0$ is valid for the high energy exchange as well. With this in mind the exchange constants can be

(34) Schlecht, S.; Hartwig, J. F. *J. Am. Chem. Soc.* **2000**, *122*, 9435–9443.
(35) Shimada, S.; Batsanov, A. S.; Howard, J. A. K.; Marder, T. B. *Angew. Chem., Int. Ed.* **2001**, *40*, 2168–2171.
(36) Montiel-Palma, V.; Lumbierres, M.; Donnadieu, B.; Sabo-Etienne, S.; Chaudret, B. *J. Am. Chem. Soc.* **2002**, *124*, 5624–5625.
(37) Lam, W. H.; Shimada, S.; Batsanov, A. S.; Lin, Z.; Marder, T. B.; Cowan, J. A.; Howard, J. A. K.; Mason, S. A.; McIntyre, G. J. *Organometallics* **2003**, *22*, 4557–4568.
(38) Hartwig, J. F.; Cook, K. S.; Hapke, M.; Incarvato, C. D.; Fan, Y.; Webster, C. E.; Hall, M. B. *J. Am. Chem. Soc.* **2005**, *127*, 2538–2552.
(39) Marks, T. J.; Shimp, L. A. *J. Am. Chem. Soc.* **1972**, *94*, 1542–1550.
(40) Beall, H.; Bushweller, H. *Chem. Rev.* **1973**, *73*, 465–486.
(41) Knizek, J.; Nöth, H. *J. Organomet. Chem.* **2000**, *614*, 168–187.

modeled at only the temperatures of coalescence, allowing for rudimentary values of $\Delta H^{\ddagger}$ to be calculated. Using these assumptions, the coalescence event observed at 196 K corresponds to a $\Delta H^{\ddagger} \approx 9 \pm 1$ kcal mol^{-1} and the event at 304 K corresponds to a $\Delta H^{\ddagger} \approx 14 \pm 1$ kcal mol^{-1}.

An excellent discussion of the binding mode for the similar complex, Cp*Ir monoboryl trihydride, is given by Hartwig and Kawamura.[42] The nomenclature question for complex **2** is confounded by the highly fluxional environment near the metal center. The line shape of the proton NMR spectrum, even at low temperature, is dominated by fluxionality, and relative broadening of the proton resonances as a result of proximity to the boron nucleus is unresolved. The ^{11}B NMR shift at 37 ppm is consistent with a σ-borane metal complex.[35,36,38]

Complex **3** can be generated quantitatively by submitting **2** to dynamic vacuum for a period of several hours. The ^{1}H NMR spectrum contains a broad singlet corresponding to one proton in the high field region indicating that product formation results from the loss of H_2. This resonance sharpens considerably in the ^{1}H{^{11}B} NMR spectrum, indicating that this proton is closely associated with a boron atom. Crystals of **3** suitable for X-ray diffraction were obtained by slow evaporation of a THF solution. The structure obtained is shown in Figure 3. Selected relevant interatomic distances and bond angles derived from X-ray diffraction data are summarized in the Supporting Information.

The structure obtained is consistent with the ^{1}H NMR spectrum of the molecule. The hydridic proton was located using Fourier difference maps and freely refined. The Ir−B distance of 2.082(5) Å is an ambiguous means to characterize the ligand environment as a boryl hydride as opposed to a σ-borane complex; however, the proximity of the hydrogen atom to both the iridium and boron atoms indicates the existence of a three-center two-electron bond (a σ-borane complex). Likewise, the location of the ^{11}B NMR shift (29.7 ppm) as well as the observation that the proton resonance at −13.16 ppm sharpens significantly upon ^{11}B decoupling are consistent with a σ-borane formulation.

When equimolar amounts of (*t*BuPOCOP)IrH_2 and 9-BBN are reacted in THF, an equilibrium is established between the reactants and the new complex **4.** This equilibrium was observed at various temperatures by NMR to give the van 't Hoff plot shown in the Supporting Information. Using this plot we calculated thermal parameters for the formation reaction. The values of $\Delta S^{\circ} = -9.1 \pm 0.5$ cal K^{-1} mol^{-1} and $\Delta H^{\circ} = -5.8 \pm 0.3$ kcal mol^{-1} are reasonable for this type of interaction.

The room temperature NMR spectra of complex **4** are remarkably similar to that of the low temperature (240 K) spectra of complex **1**. They both display two broad resonances corresponding to protons bound to boron and one sharp resonance with well defined coupling corresponding to an Ir-bound proton in the high field region of the ^{1}H spectra. Both Ir bound protons exhibit scalar coupling to the more downfield of the two B bound protons. Given these similar spectroscopic features it is also quite possible that both complexes have similar binding geometries near the Ir center. The fact that well resolved features for **1** are only seen at low temperatures is likely due to the ability of the BH_3 ligand to exchange hydrogen positions in a manner not possible for the 9-BBN ligand. It is also likely that complete formation of **4** is prevented by the much bulkier 9-BBN ligand.

Conclusions

The geometric arrangement of the atoms in compound **1** appears to consist of a highly asymmetric η^2 binding mode of a tetrahydroborate ligand with the most highly activated B−H bond, 1.74(5) Å, reported in the literature to date. However, while there is spectroscopic evidence for a significant interaction between B1 and H2, we feel that the distance of 1.74(5) Å is too long to be considered a covalent bond, thus precluding characterization of compound **1** as a tetrahydroborate complex. Rather, complex **1** may be considered the first well characterized example of a transition metal σ complex of borane, with an activated B−H bond distance of 1.45(5) Å. As the starting material may consist of $NaBH_4$, this complex is of particular interest when considered as a model for methane activation.[43,44]

Compounds **2** and **3** are closely analogous to other complexes that have displayed stoichiometric and catalytic functionalization of alkanes.[38,42,45,46] It is therefore of great interest to explore the reactivity of the present compounds, given their previously shown potential for dehydrogenation reactions as well as their high thermal stability as catalysts.

Experimental Section

General Considerations. Unless otherwise stated, all manipulations were carried out using high vacuum techniques or under an atmosphere of argon in a glovebox (Vacuum Atmospheres) or using Schlenk techniques. THF was purified by passage through a column of alumina, and pentane and heptane through columns of alumina and Q5 reactant. THF-d_8 was vacuum transferred from sodium metal/benzophenone.

Solution NMR spectra were collected at room temperature unless otherwise specified using Bruker AV500 and DRX500 spectrometers. ^{1}H, ^{2}H and ^{13}C{^{1}H} NMR spectra were referenced to residual solvent signals and shifts are reported in parts per million (ppm) downfield of tetramethylsilane. ^{31}P{^{1}H} NMR spectra were referenced to an external H_3PO_4 (85%) sample set to 0 ppm and ^{11}B NMR spectra to an external sample of neat $BF_3 \cdot Et_2O$ set to 0 ppm. Infrared spectra were recorded on a Bruker Optics Tensor27 FT-IR spectrometer at room temperature. Relaxation rate (T_1) experiments were conducted using a saturation recovery pulse sequence (180–τ–90). Temperature measurements for variable temperature experiments were calibrated using a sample of neat methanol.

NaH was purchased from Aldrich as a dispersion in mineral oil and rinsed with hexanes prior to use. 9-BBN was purchased from ACROS Organics and recrystalized from hexanes prior to use. HBpin was purchased from Aldrich and vacuum distilled immediately prior to use. Complexes (*t*BuPOCOP)IrHCl,[6] (*t*BuPOCOP)IrH_2,[7] sodium dihydro-9-boratobicyclononane,[41] **1**,[9] and **1-*d*$_4$**,[9] were prepared according to literature procedures.

(POCOP)IrH_3Bpin (2). A 23 mM solution of HBpin in THF-d_8 was prepared and stored at −20 °C. (*t*BuPOCOP)IrH_2 (11 mg, 19 μmol) was weighed into a J. Young NMR tube. The chilled solution of HBpin (1.2 mL, 28 μmol) was added to the tube at a temperature of $\approx$ −20 °C and shaken briefly to give an orange solution. The tube was transferred via a dry ice/acetone bath immediately to a precooled NMR probe. NMR spectra show nearly (>99%) quantitative conversion to product in solution. Complex **2** decomposes at room temperature to give complex **3** and H_2. ^{1}H NMR (170 K, THF-d_8, 500 MHz) δ 6.7 (t, 1 H, J = 8 Hz, H4); 6.4

(42) Hartwig, J. F.; Kawamura, K. *J. Am. Chem. Soc.* **2001**, *123*, 8422–8423.
(43) Hall, C.; Perutz, R. N. *Chem. Rev.* **1996**, *96*, 3125–3146.
(44) Makhaev, V. D. *Russ. Chem. Rev.* **2003**, *72*, 257–278.
(45) Chotana, G. A.; Rak, M. A.; Smith, M. R., III *J. Am. Chem. Soc.* **2005**, *127*, 10539–10544.
(46) Smith, M. R., III *Prog. Inorg. Chem.* **1999**, *48*, 505–567.

(d, 2H, $J = 8$ Hz, H3,5); 1.5 (br s, 18H, *t*Bu); 1.3 (br s, 18H, *t*Bu): 1.2 (s, 12H, Me); −8.1 (s br, 1H, B*H*Ir); −9.7 (s br, 1H, Ir*H*): −10.2 (s br, 1H, Ir*H*), (242 K, THF-d_8, 500 MHz) δ 6.66 (t, 1 H, $J = 7.8$ Hz, H4); 6.36 (d, 2H, $J = 7.8$ Hz, H3,5); 1.44 (br s, 18H, *t*Bu); 1.32 (br s, 18H *t*Bu): 1.22 (s, 12H, Me); −8.0 (s br, 1H, B*H*Ir); −10.0 (s br, 2H, Ir*H*), (335 K, THF-d_8, 500 MHz) δ 6.66 (t, 1 H, $J = 7.8$ Hz, H4); 6.35 (d, 2H, $J = 7.8$ Hz, H3,5); 1.40 (virtual triplet, 36H, apparent $J = 7$ Hz, *t*Bu); 1.22 (s, 12H, Me); −9.3 (s br, 3H, Ir*H*). $^{31}P\{^1H\}$ NMR (THF-d_8, 202 MHz) δ 173.9 (s). $^{11}B\{^1H\}$ NMR (THF-d_8, 160 MHz) δ 37 (s br).

(POCOP)IrHBpin (3). HBpin (29 mg, 230 μmol) was weighed into a vial and 2 mL of THF was added. (*t*BuPOCOP)IrH_2 (0.10 g, 170 μmol) was weighed into a vial and 2 mL of THF was added to give a red solution. Both solutions were chilled to ≈ -20 °C before being added together and stirred briefly to give an orange solution and then transferred to an ice bath. Solvents were removed under vacuum at 0 °C and the product was kept under dynamic vacuum (<5 mTorr) for 24 h at room temperature to yield a dark orange solid. Crystals suitable for X-ray diffraction were obtained by slow evaporation of a THF solution. ^1H NMR (THF-d_8, 500 MHz) δ 6.90 (t, 1 H, $J = 8$ Hz, H4); 6.54 (d, 2H, $J = 8$ Hz, H3,5); 1.38 (virtual triplet, 36H, apparent $J = 7$ Hz, *t*Bu); 1.22 (s, 12H, Me); −13.15 (s br, 1H, Ir*H*B). $^1H\{^{11}B\}$ NMR (THF-d_8, 500 MHz) as ^1H except δ −13.15 (t, $J_{HP} = 5$ Hz, Ir*H*B). $^{31}P\{^1H\}$ NMR (THF-d_8, 202 MHz) δ 192.8 (s). $^{11}B\{^1H\}$ NMR (THF-d_8, 160 MHz) δ 29 (s br). IR (KBr, cm^{-1}) 2014 (ν_{BH}).

(POCOP)IrH_3-9-BBN (4). (*t*BuPOCOP)IrH_2 (21 mg, 35 μmol) and 9-BBN (4.1 mg, 33 μmol) were weighed into a J. Young NMR tube. THF-d_8 was vacuum transferred into the tube to give a light red solution upon shaking. ^1H NMR (THF-d_8, 500 MHz) δ 6.67 (t, 1 H, $J = 8$ Hz, H4); 6.38 (d, 2H, $J = 7$ Hz, H3,5); 2.0 - 1.5 (m, br, 14H, BBN); 1.42 (virtual triplet, 18H, apparent $J = 7$ Hz, *t*Bu); 1.35 (virtual triplet, 18H, apparent $J = 7$ Hz, *t*Bu); 1.22 (s, 12H, Me); −6.0 (s br, 1H, Ir*H*B); −7.4 (s br, 1H, Ir*H*B); −21.32 (dt, $J = 12$ Hz, 1H, Ir*H*. $^{31}P\{^1H\}$ NMR (THF-d_8, 202 MHz) δ 171.5 (s). $^{11}B\{^1H\}$ NMR (THF-d_8, 160 MHz) δ 30. (s br).

Neutron Diffraction Study of Complex 1. Neutron diffraction data were obtained at the Intense Pulsed Neutron Source (IPNS) at Argonne National Laboratory using the time-of-flight Laue single-crystal diffractometer (SCD)[47,48] At the IPNS, pulses of protons are accelerated into a depleted uranium target 30 times a second to produce pulses of neutrons by the spallation process. Exploiting the pulsed nature of the source, neutron wavelengths are determined by time-of-flight based on the de Broglie equation $\lambda = (\hbar/m) \cdot (t/l)$, where $\hbar$ is Planck's constant, m is the neutron mass, and t is the time-of-flight for a flight path l, so that the entire thermal spectrum of neutrons can be used. With two position-sensitive area detectors and a range of neutron wavelengths, a solid volume of reciprocal space is sampled with each stationary orientation of the sample and the detectors. The SCD has two ^{6}Li-glass scintillation position-sensitive area detectors, each with active areas of 15 × 15 cm^2 and a spatial resolution of <1.5 mm. One of the detectors is centered at a scattering angle of 75° and a crystal-to-detector distance of 23 cm, and the second detector is at 120° and 18 cm. Details of the data collection and analysis procedures have been published previously.[49]

A crystal of (POCOP)$Ir(H)_2(BH_3)$ (**1**), with approximate dimensions of 4 × 3 × 0.5 mm^3 and a weight of 10 mg, was coated in fluorocarbon grease under inert atmosphere, wrapped in aluminum foil and glued to an aluminum pin that was mounted on the cold stage of a closed-cycle helium refrigerator. The crystal was then cooled to 30 ± 1 K. For each setting of the diffractometer angles, data were stored in three-dimensional histogram form with coordinates *x,y,t* corresponding to horizontal and vertical detector positions and the time-of-flight, respectively. An autoindexing algorithm[50] was used to obtain an initial orientation matrix from the peaks in three preliminary histograms measured for 60 min each. This unit cell approximately matched the previously reported X-ray unit cell indicating that the neutron sample was the correct material.[9] For intensity data collection, runs of 6 h per histogram were initiated for the data set. Settings were arranged at χ and ϕ values suitable to cover at least one unique hemisphere of reciprocal space (Laue symmetry –1). With the above counting times, 22 histograms were completed in the 6 days available for the experiment. Bragg peaks in the recorded histograms were indexed and integrated using individual orientation matrices for each histogram, to allow for any misalignment of the sample. Intensities were integrated about their predicted locations and were corrected for the Lorentz factor, the incident spectrum, and the detector efficiency. A wavelength-dependent spherical absorption correction was applied using cross sections from Sears[51] for the nonhydrogen atoms and from Howard and co-workers[52] for the hydrogen atoms (μ (cm^{-1}) = 1.692 + 2.400 λ). Symmetry-related reflections were not averaged since different extinction factors are applicable to reflections measured at different wavelengths.

The structure model was refined using the GSAS software package.[53] The atomic positions of the X-ray diffraction structure, except for the hydride ligands on iridium, were used as a starting point in the refinement. Hydrogen atoms around iridium and boron were clearly located in difference Fourier maps. Disorder in the *t*butyl ligands was left unmodeled. The refinement was based on F^2 reflections with a minimum d-spacing of 0.9 Å. Weights were assigned as $w(F_o^2) = 1/\sigma^2(F_o^2)$ where $\sigma^2(F_o^2)$ is the variance based on counting statistics. In the final refinement all atoms, including hydrogen atoms, were refined with isotropic displacement parameters. Due to the high background and low number of data greater than 3σ, an anisotropic refinement was not possible and the uncertainties of bond distances and angles are quite large. Data collection and refinement parameters are summarized in the Supporting Information.

X-Ray Diffraction Study of Complex 3. An orange prism, 0.59 × 0.40 × 0.38 mm in size was mounted on a glass capillary with oil. Data were collected at −143 °C on a Nonius FR590 Kappa CCD X-ray spectrometer. The crystal-to-detector distance was 30 mm and exposure time was 15 s per degree for all sets. The scan width was 1°. Data collection was 88.1% complete to 31.97° and 99.9% complete to 25° in ϑ. A total of 114020 partial and complete reflections were collected covering the indices, $h = -61$ to 61, $k = -16$ to 16, $l = -21$ to 21. 10236 reflections were symmetry independent and the $R_{int} = 0.0974$ indicated that the data was of average quality. Indexing and unit cell refinement indicated a monoclinic *C* lattice. The space group was found to be *C*2/*c* (No. 15).

The data were integrated and scaled using hkl-SCALEPACK.[54,55] This program applies a multiplicative correction factor (S) to the observed intensities (I) and has the following form:

$$S = (e^{-2B(\sin^2\theta)\lambda^2})/\text{scale}$$

S is calculated from the scale and the B factor determined for each frame and is then applied to I to give the corrected intensity (I_{corr}).

(47) Schultz, A. J.; Srinivasan, K.; Teller, R. G.; Williams, J. M.; Lukehart, C. M. *J. Am. Chem. Soc.* **1984**, *106*, 999–1003.
(48) Schultz, A. J. *Trans. Am. Crystallogr. Assoc.* **1987**, *23*, 61–69.
(49) Schultz, A. J.; Van Derveer, D. G.; Parker, D. W.; Baldwin, J. E. *Acta Cryst. C* **1990**, *46*, 276–279.
(50) Jacobson, R. A. *J. Appl. Crystallogr.* **1986**, *19*, 283–286.
(51) Sears, V. F. In *Methods of Experimental Physics*; Vol. 23, Neutron Scattering, Part A; Academic Press: Orlando, FL, 1986; p 521–550.
(52) Howard, J. A. K.; Johnson, O.; Schultz, A. J.; Stringer, A. M. *J. Appl. Crystallogr.* **1987**, *20*, 120–122.
(53) Larson, A. C.; Von Dreele, R. B. *General Structure Analysis System-GSAS*; Los Alamos National Laboratory: Los Alamos, NM, 2000.
(54) Otwinowsky, Z.; Minor, W. *Methods Enzymol.* **1997**, *276*, 307–326.
(55) Mackay, S.; Edwards, C.; Henderson, A.; Gilmore, C.; Stewart, N.; Shankland, K.; Donald, A. *MaXus*; University of Glasgow: Scotland, 1997.

Solution by direct methods (DIRDIF)[56] produced a complete heavy atom phasing model consistent with the proposed structure. All hydrogen atoms were located using a riding model. All non-hydrogen atoms were refined anisotropically by full-matrix least-squares emploing SHELXL-97.[57] Scattering factors are from Waasmair and Kirfel.[58] Graphics were produced by ORTEP for Windows.[59] A disordered solvent molecule, THF, was found with two molecules sharing one THF. The thermal properties of the THF were restrained via a model that assumes similar thermal properties along chemical bonds.

Approximating the electron density distribution by a sphere, as is only possible with the present software, leaves distinct electron density maxima around the Ir core of the complex halfway between the bonds of Ir to P, B and C. In addition to these were two small electron densities on both sides of the coordination plane through P, C and Ir at distances of 1.931 Å and 1.967 Å. One distinct electron density appeared at an angle similar to that of the distortion of B from the coordination plane at a distance of 1.555 Å. A hydrogen atom (H1) was assigned to this larger electron density and freely refined. The thermal coefficient was found to match that of the Ir and B atoms confirming a correct assignment.

Acknowledgment. This work was supported by the U.S. Department of Energy (DOE) as part of the Center of Excellence for Chemical Hydrogen Storage. Partial support (D.M.H.) was provided by the National Science Foundation. Work at Argonne National Laboratory was supported by the DOE, Office of Science, Basic Energy Sciences, under contract DE-AC02-06CH11357.

Supporting Information Available: CIF files for **1** and **3** and an IR spectrum of **1**. Experimental details for the location of H atoms and neutron diffraction data collection of **1**. This information is available free of charge via the Internet at http://pubs.acs.org.

JA801898M

(56) Beurskens, P. T.; Admiraal, G.; Beurskens, G.; Bosman, W. P.; García-Granda, S.; Gould, R. O.; Smits, J. M. M; Smykalla, C. *The DIRDIF96 Program System*; Technical Report of the Crystallography Laboratory; University of Nijmegen: The Netherlands, 1996.
(57) Sheldrick, G. M. *SHELXL97*; University of Göttingen, Germany, 1997.
(58) Waasmaier, D; Kirfel, A. *Acta Cryst. A.* **1995**, *51*, 416.
(59) Farrugia, L. J. *Appl. Cryst.* **1997**, *30*, 565.